J Appl Biotechnol Rep. 2023 September;10(3):1091-1097

Journal of
Applied Biotechnology Reports

doi 10.30491/JABR.2023.375829.1584

Original Article

Detection of Shiga-like Toxin Produced by *E. coli* O157:H7 based on the LSPR Property of Gold Nanoparticles

Fatemeh Yaghoubi [1], **Mehdi Zeinoddini** [1*], **Mohammad Shoushtari** [2]

[1] Faculty of Chemistry and Chemical Engineering, Malek Ashtar University of Technology, Iran
[2] Department of Virology, Pasteur Institute of Iran, Tehran, Iran

Corresponding Author: Mehdi Zeinoddini, PhD, Associate Professor, Faculty of Chemistry and Chemical Engineering, Malek Ashtar University of Technology, Iran. Tel: +98-2122974600, E-mail: zeinoddini52@mut.ac.ir

Received December 7, 2022; **Accepted** March 11, 2023; **Online Published** September 10, 2023

Abstract

Introduction: Shiga-like toxin-producing *E. coli* (STEC) was first introduced as a human pathogen in 1982. STEC serotypes were isolated from animals, foods, and other samples. This serotype is the leading cause of single and epidemic Hemorrhagic colitis and Haemolytic uremic syndrome. STEC serotype produces two potent toxins named Shiga-like toxin 1 and 2, whose genomes are encoded by phage. These toxins have a cytopathic effect on intestinal epithelial cells that cause bloody diarrhea. This study aimed to design and evaluate a nanobiosensor based on the LSPR (Local Surface Plasmon Resonance) property of citrated gold nanoparticles (GNP), by modifying the pH of the GNP environment and conjugation (non-covalent bonding) of GNP with rabbit anti- Shiga-like toxin polyclonal antibody (IgG).

Materials and Methods: In this process, the binding of gold nanoparticles to antibodies and the detection of Shiga-like toxin were confirmed using UV-visible and DLS methods and the sensitivity and specificity of the produced nanobioprobe were evaluated using the ELISA method.

Results: The results showed that the sensitivity of this method in detecting Shiga-like toxin is about 10 ng/ml and the visible color-changing of the nanoprobe suspension was confirmed for all vials containing the target antigen in less than 1 h.

Conclusions: In conclusion, the advantage of the produced nanobioprobe over other methods is the detection of small quantities of analytes, low cost, and detection in less than 2 h.

Keywords: *E. coli* O157:H7, Shiga-like Toxin, Polyclonal Antibody, Gold Nanoparticles, LSPR

Citation: Yaghoubi F, Zeinoddini M, Shoushtari M. Detection of Shiga-like Toxin Produced by *E. coli* O157:H7 based on the LSPR Property of Gold Nanoparticles. J Appl Biotechnol Rep. 2023;10(3):1091-1097. doi:10.30491/JABR.2023.375829.1584

Introduction

Escherichia coli is a member of the *Enterobacteriaceae* family, the largest family of Gram-negative bacteria, and belongs to the genus *E. coli*, Enterotoxigenic virotype (ETEC). *E. coli* O157:H7 is the most critical strain that produces Shiga-like toxins and is involved in foodborne illnesses.[1] *E. coli* O157:H7 infection often occurs with contaminated beef, raw milk, and other cow products.[2] *E. coli* infections are common in different countries of the world. For example, according to the Centers for Disease Control (CDC), there have been 73,000 cases of *E. coli* infections in the United States. The ability of *E. coli* O157: H7 to cause several diseases in humans is due to the release of Shiga-like toxins (Stx1 and Stx2) or verocytotoxin.[3] Another causative agent is the 94-KDa outer membrane protein called intimin, which binds bacteria to the intestine that is encoded by the *eaeA* gene. The third factor that may be involved in the pathogenicity of *E. coli* O157:H7 is Enterohemolysin (Ehly), which is encoded by the *hly* gene.[4] In addition to the genes encoding Shiga-like toxins (Stx1 and Stx2), as well as *eaeA* and *hly* genes, which are the most known pathogenic genes in STEC strains, *E. coli* O157:H7 has two specific antigens, O-polysaccharide (O157) and flagellum protein (H7). Evaluation of *rfb* O157 and *flic* H7 genes with antiserum can help to more accurately diagnose this pathogen.[5] On the other hand, Shiga toxins belong to a large family of bacterial toxins that are mainly produced by *Shigella dysentery* serotype 1 and the STEC pathotypes, such as *E. coli* O157:H7, which can cause disease.[6] Also, these toxins belong to the AB family of protein toxins. Part B is the pentameric and non-toxic subunit, which specifically binds to the target cell surface via a glycolipid receptor called Gb3. Then the catalytic part A enters the cytosol and inhibits the protein synthesis in the host cell by removing one adenine from 28S rRNA subunits of 60S ribosomes, leading to cell death. In some cells, this toxin also synthesizes cytokines and induces apoptosis by ribotoxic stress.[7] In addition, Shiga-like toxins increase the signaling cascade and activity. So far, different types of this toxin have been identified, including Stx2f, Stx2, Stx2c, Stx2d, Stx2e, Stx1, Stx1c, and Stx2.[8] Biosensors are analytical devices that are able to detect the type and concentration of an analyte, and then, the detected analyte is converted into

electrical, optical, and similar signals using converters. In metal nanoparticles, surface plasmon resonance (SPR) is responsible for the emergence of their unique optical properties. The first use of surface plasmon resonance was made in 1990, and since then, SPR has been recognized as one of the optical biosensor technologies in various fields of chemistry, biology, and medicine.[9-11] The phenomenon of surface plasmon resonance, excitation, and mass vibration of free electrons is a common boundary between metal and dielectric. Arousal is caused by the interaction of electromagnetic waves in the visible region with the plasmons of the gold and silver nanoparticle conductive layer. The use of nanoparticles as a label is due to the high sensitivity of nanoparticles to changes in the coefficient of failure of the environment around them. Gold and silver nanoparticles have a strong absorption peak in the visible region and are easily operated by accepting molecules, so they are the best choice as a label.[12] In this method, the plasmon response of the nanoparticle conduction layer to the electromagnetic field in the presence of biomolecules can be observed by displacement at wavelength and reduction of adsorption. By binding antibody to GNP, red shift occurs, because the refractive index in the presence of an antibody is larger than that of the surrounding environment. When large molecules, such as biomolecules are placed on the surface, they occupy more volume, resulting in an increase in LSPR wavelength shift.[13] In this work, we designed and evaluated a nanobioprobe using the LSPR properties of GNP, for detection of *E. coli* O157:H7.

Materials and Methods

$NaPO_4$ buffer**,** chloroauric acid ($HAuCl_4$), sodium citrate, K_2CO_3, NaCl, bovine serum albumin (BSA), phosphate-buffered saline (PBS) tablets, Tween-20, TMB, and H_2SO_4 were purchased from Merck (Sigma-Aldrich). Other chemicals were provided from Merck (Kenilworth, NJ).

Antibody Purity and Concentration

Polyclonal anti-Shiga-like toxin (IgG) and Shiga-like toxin were prepared from our previous investigation (data not reported). To determine the purity of IgG, this antibody was analyzed using SDS-PAGE method on a 10% acryl amid and stained with coomassie brilliant blue, and then, the concentration was determined using Bradford method.

Synthesis of 40-nm Spherical Gold Nanoparticles

We used Turkovitch's method to synthesize GNP.[14] To obtain 10 ml of gold nanoparticles, 10 ml of deionized water was put in an erlenmeyer flask on the magnetic stirrer to boil. 100 µl of 1% $HAuCl_4$ solution was added to boiling deionized water on the stirrer. Then, 100 µl of 1% sodium citrate was added to the solution and the process continued until the red color appeared. In following, the red solution was placed on the ice to cool completely. GNPs were characterized applying transmission electron microscopy (TEM), dynamic light scattering (DLS), and zeta potential (Zp), to determine size distributions, the electrical surface charge and size, respectively. Also, the formation of spherical gold nanoparticles was determined by a UV-visible spectrophotometer (Amersham Biosciences4300 Amersham BioSciences UK Ltd., Buckinghamshire, UK), and recorded in the wavelength range of 400-700 nm.

Conjugation of GNP with Antibodies (Physical Interactions)

Firstly, to determine the appropriate IgG concentration, 25 µl of antibody at the concentrations of 0, 1, 3, 5, and 7 µg/ml was added into a 96-well plate. The pH of GNPs was set to 9 using K_2CO_3 solution (GNPs pH was higher than the isoelectric pH); then, 125 µl of GNP was added to each well and after 5 minutes of incubation, 125 µl of NaCl solution was added to each well. At a lower concentration of antibody (for conjugation), sodium salt attaches to the free space around the GNPs (not attached to the antibody) and neutralizes the charge around the nanoparticles and it changes color from red to blue. In following, the antibody with a specific concentration was added to 300 µl of GNP with pH 9, and incubation was done for 1 h on the ice. After that, 30 µl of 10% BSA was added and the solution was incubated for 20 minutes (to block the empty spaces around the GNPs). To remove excess BSA and antibodies that were lost attached, the centrifuge process was performed for 20 minutes at 12000 rpm and 4 °C. After that, the supernatant was removed and the pellet was dissolved in distilled water with a volume of 300 µl. Finally, to confirm the conjugation (physical interaction), the changes of the UV-visible absorbance (the LSPR band) of GNPs before and after the conjugation were analyzed using the DLS and UV-visible techniques.

Immunological Activity and Specificity of Nanobioprobe

To evaluate the sensitivity of the nanobioprobe in the presence of various concentrations of Shiga-like toxin, a serial dilution of 0, 10, 100, 300, 500, and 700 ng was prepared from Shiga-like toxin in 300 µl of the nanobioprobe and incubated on ice for 1 h. The solution was then centrifuged at 12000 rpm and 4 °C for 4 min. Then the change in color of vials at optical detection and LSPR wavelength was investigated by UV-visible technique. In addition, the activity of IgG before and after bioconjugation was monitored using conventional ELISA. For this purpose, serial dilutions of Shiga-like toxin (from 0 to 1000 ng) and a negative sample (M2 Protein extracted from influenza virus) were coated in 2 rows of a 96-well plate and incubated at 4 °C for 24 h, then the wells were washed three times with PBS-T (phosphate-buffered saline with Tween-20). At the next step, 100 µl of IgG was added to the first rows and 100

µl of the nanobioprobe in the second row, and the plate was incubated at 4 °C for 1 h. The three-time washing with PBS-T was repeated. Then the second antibody conjugated with horseradish peroxidase (HRP) was added and the plate was incubated at 4 °C for 1 h. Finally, after the wash, a substrate solution (TMB and H_2O_2) was added and the plate was kept in the dark place until the appearance of the color. The results were recorded by an ELISA reader at the wavelengths of 450 and 630 nm, after stop reaction (by 0.5 M of H_2SO_4).

Results

Characterization of IgG

To determine the purity and concentration of IgG, this antibody was tested on a 10% polyacrylamide gel electrophoresis (Figure 1) and Bradford method. The result of SDS-PAGE showed a suitable purity (about 90%, 150 kDa, using *ImageJ* software) and the protein concentration was estimated to be 1 mg/ml.

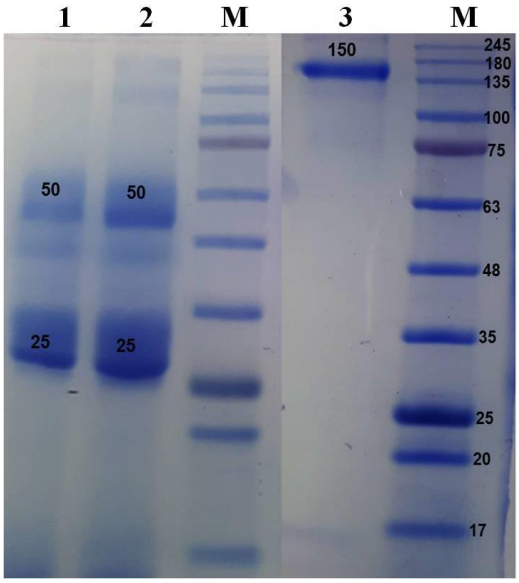

Figure 1. SDS PAGE Analysis Reducing **(1, 2)** and Non-reducing **(3)** of Anti- *E. coli* O157:H7 Purified IgG. **(M)** Protein Size Marker.

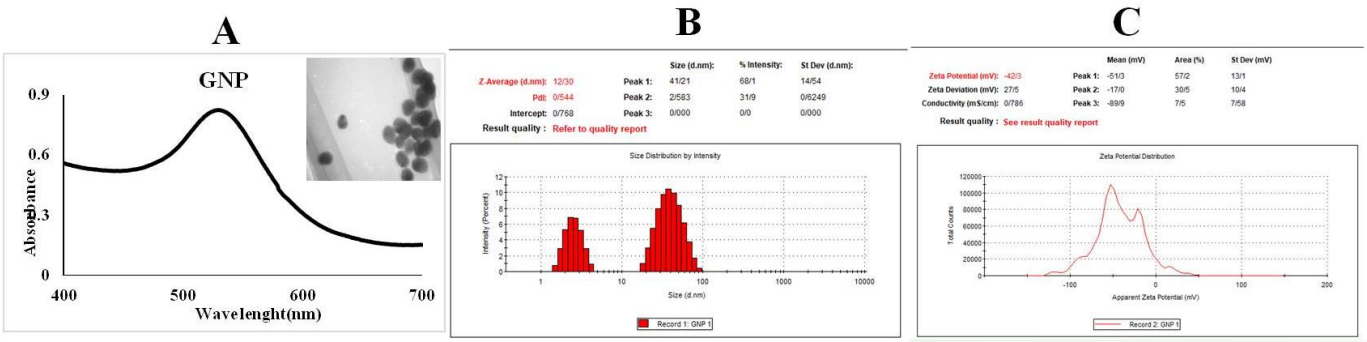

Figure 2. The Properties and Characteristics of Synthesized GNPs. **(A)** UV-visible absorption spectra of GNPs in the range of 400-700 nm, (the upper part) visual observation of GNPs using TEM; **(B)** Results of the DLS for the GNP size, and **(C)** The DLS for the zeta potential of the GNP concentration of IgG to make the nanobioprobe.

Characterization of Gold Nanoparticles

A fast and inexpensive way to ensure the synthesis of spherical gold nanoparticles and to evaluate the absorption spectra of plasmonic nanoparticles is using a spectrophotometer and UV-Visible spectroscopy. In this method, gold spherical nanoparticles have an absorption peak and absorb a wavelength of 530 nm. In this study, the absorption intensity of nanoparticles was examined in the wavelength range of 700-400 nm. According to the obtained diagram, spherical gold nanoparticles have a strong absorption peak at 530 nm (Figure 2A). On the other hand, the TEM picture showed that, the gold colloid solution is in a suspension condition, according to the negatively charged layer of citrate ions that redirect atoms from each other and the maximum shape of the gold nanospheres was globular and around 40 nm in size (Figure 2A-the upper part). In addition to this method, we used the DLS technique to measure the size and zeta potential (charge) of gold nanoparticles, that approximately 70% of the synthesized nanoparticles had a size of 41 nm and a charge of about -51 (Figure 2B and 2C).

The Nanobioprobe Production

The appropriate concentration of IgG for conjugation was determined by its aggregation in NaCl salt. According to figure 3A, IgG did not aggregate at the concentrations of 5 and 7 µg/ml. This indicates that the minimum concentration of antibodies, which can surround the nanoparticles is 5 µg/ml, so there is no empty space for salt binding at 5 µg/ml. Therefore, a concentration of 5 µg/ml was used (Figure 3A). Also, according to Figure 3B, the absorption peak of nanobioprobe decreased compared to GNP, and the LSPR bandwidth was regularly shifted to higher areas (red shift). These results indicate the conjugation of the antibody to the gold nanoparticles. Because the LSPR band of GNP is directly related to its surface mass, the surface mass of nanoparticles increases with increasing antibody concentration,

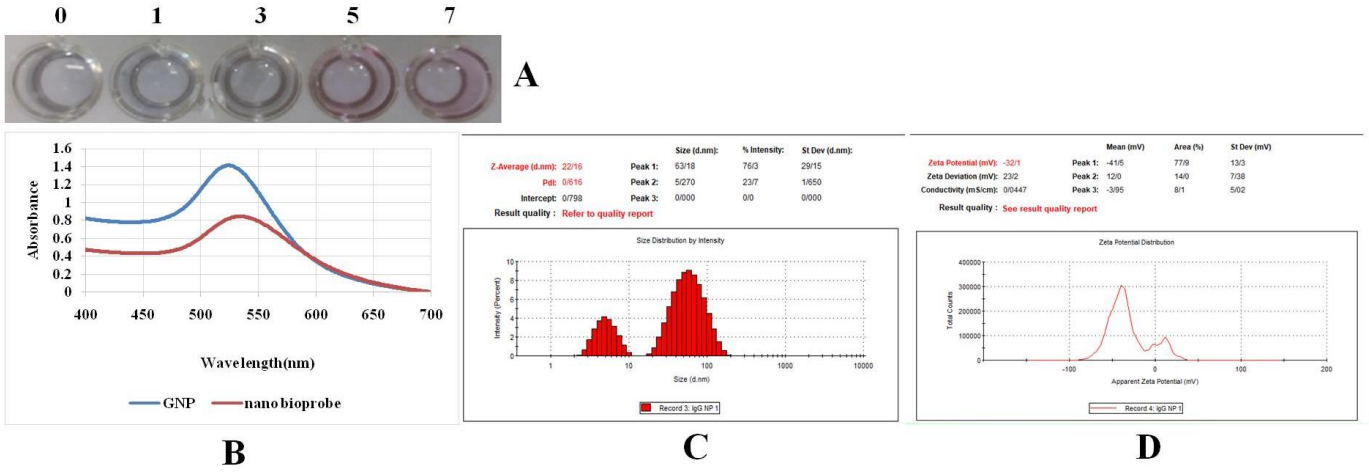

Figure 3. (A) IgG color changes at the concentrations of 0 to 5 µg/ml with gold spherical nanoparticles in the presence of NaCl salt; **(B)** LSPR GNP band wavelength changes after conjugation with IgG; **(C)** Results of the DLS for the size of the IgG nanoprobe, and **(D)** The DLS for the IgG nanoprobe zeta potential.

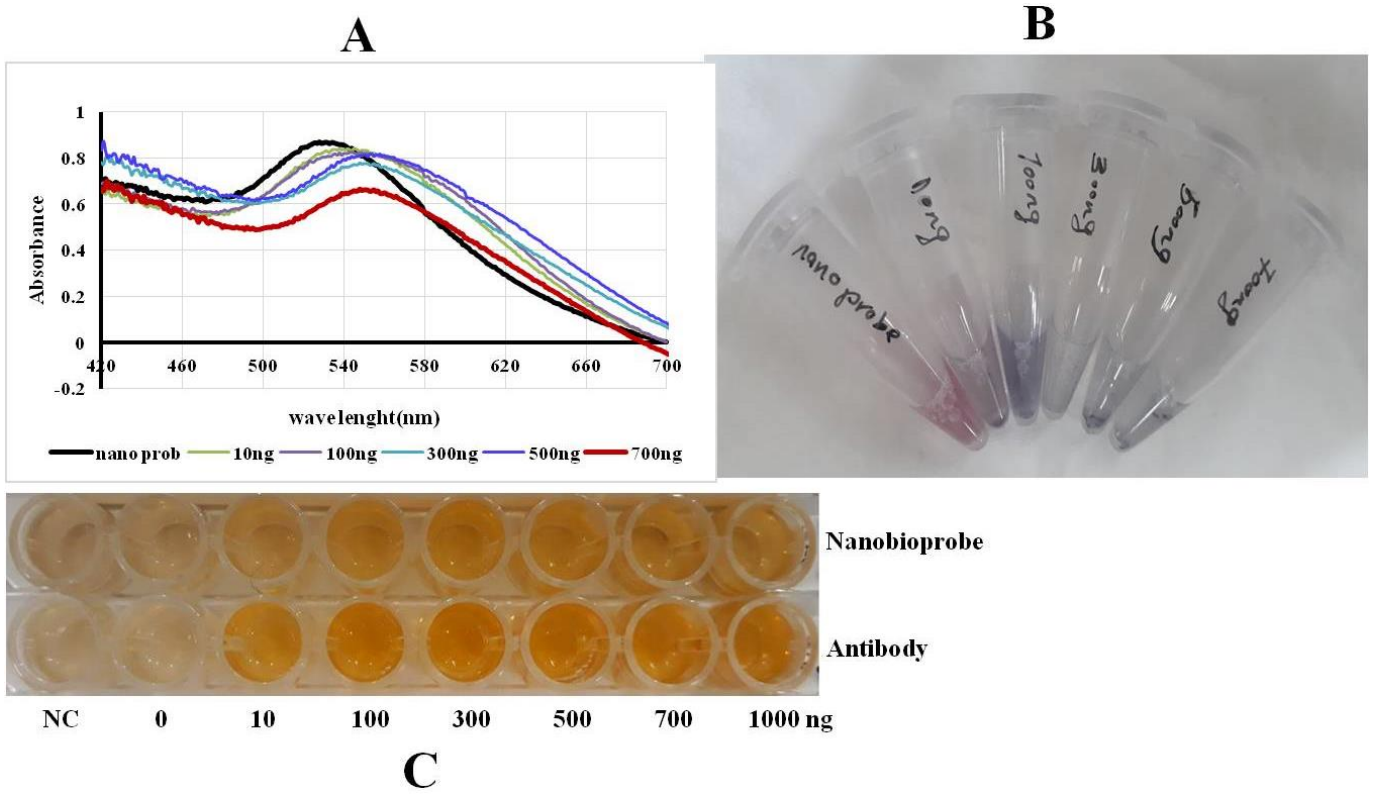

Figure 4. (A) The alteration of LSPR GNP conjugated to IgG antibody absorption band at different bacterial concentrations; **(B)** Visual nanobiprobe color changing at different concentrations of toxin from 0 to 700 ng; **(C)** Comparison of the optical results of ELISA using IgG antibody before and after conjugation with GNP.

and the LSPR wavelength shifts to red areas. Another way to confirm the formation of nanobioprobes is DLS. As shown in the comparison of Figure 3D/3E and Figure 2B/2C, the size of the surface charge from nanobioprobe has relatively increased.

Performance of the Nanobioprobe LSPR

According to the results of the study of changes in the LSPR band of nanobioprobe in figure 4A, in the presence of Shiga-like toxin, the LSPR band of nanobioprobe made is moved to a higher wavelength and its absorption is reduced. This displacement and reduction of adsorption were directly related to the concentration of toxin, so that in high concentrations of toxin, the absorption of nanobioprobe was greatly reduced and its absorption wavelength was shifted to a higher (red) wavelength. This shift in intensity reflects the high sensitivity

of the LSPR nanobioprobe band to changes in the environmental refractive index. In the presence of 10 ng/ml of toxin, the LSPR band of the nanobioprobe is shifted to a longer (red) wavelength, and its absorption is reduced, indicating the ability to detect Shiga-like toxin at the lowest concentration, 10 ng/ml. An important feature of the designed nanobioprobe is the ability to detect target analytes with the naked eye. After the toxin binds to the nanobioprobe (suitable concentration), the negative charges around the nanobioprobe are neutralized, thus eliminating the repulsion between the nanobioprobes and causing cumulative behavior and changing the color of the solution from red to blue. As we have shown in Figure 4B, in a microtube containing a toxin with a concentration of 10 ng/ml, color changes from red to blue are quite significant. So much so that at higher concentrations of the toxin, the accumulative behavior of the nanobioprobe causes it to aggregate, resulting in discoloration of the solution inside the microtube.

The Specificity of Nanobioprobe

The specificity of antibodies, before and after conjugation (produced nanobioprobe) was evaluated using the ELISA method. For this, indirect ELISA is used for measuring the function of a labeled antibody with GNP. As we can see in figure 4C, comparing the results of the ELISA method, the nanobioprobe with antibody without conjugate is almost the same, with the difference that the amount of antibody activity after conjugation has decreased slightly. This indicates that the nanoparticles do not bind to the antibody Fab part and do not alter the immunological function of the antibody. In the negative control well, according to no connection between the nanobioprobe and the negative control (M2 protein), the nanobioprobe is removed during the washing stage and no color change is observed, which indicates the specificity of produced nanobioprobe.

Discussion

In this study, the binding of gold nanoparticles to antibodies and the detection of Shiga-like toxin were confirmed using UV-visible and DLS methods and the sensitivity and specificity of the produced nanobioprobe were evaluated using the ELISA method. The results showed that the sensitivity of this method in detecting Shiga-like toxin is about 10 ng/ml concentration. One of the most important properties of metal nanoparticles, especially gold and silver, is their plasmonic properties. When the electrons in the capacitance are out of equilibrium, plasmonics are formed. This feature is used to build sensors in medicine and industry. Gold nanoparticles have a certain plasmon absorption frequency wavelength, which is measurable. After combining different materials with gold nanoparticles, the refractive index and wavelength of nanoparticles change, which can be seen both visually and with a measurable detector.[15]

Connecting specific molecules to the surface of nanoparticles can cause a change in the dielectric constant, which causes a change in color and visual observation of changes in the concentration of the analyte without the need for a device quantitatively (color change from red to blue in different concentrations).[9] LSPR-based sensors are resistant to electromagnetic interference and can be monitored remotely due to this resistance.[16] According to the results of this study, Shiga-like toxins can be detected in less than 2 h, which is a relatively fast time to diagnose analytics. This method is cheap, without the need for a diagnostic device. If it is made in the form of a rapid test kit, it is portable and can be used anywhere without the need for specialized personnel, and because specific antibodies have been used to identify the target, it is a highly specific detection method. The presence of gold nanoparticles and their sensitivity to environmental dielectric changes cause the high sensitivity of these sensor nanoparticles in analyzing the analytes. As reported, the sensitivity of the sensor to the Shiga-like toxin is 10 ng/ml. Other identification methods that have been used to date have shortcomings as follows. The first category is the conventional microbiological methods. In these methods, for detecting toxin-producing bacteria, food samples are cultivated in different or selective media. These methods are suitable for studying phenotype and metabolic fingerprinting, but they require a long time, an incubator, and are labor-intensive methods.[17] The second category is the traditional methods that involve various pre-enrichment, selective enrichment, biochemical screening, and serological confirmation steps. These methods are laborious and time-consuming, and require trained personnel due to the need to accurately distinguish non-pathogenic bacteria from pathogens.[18] Other traditional methods for detecting bacteria include counting cells using a microscope, flow cytometry, impedimetry, redox reactions, ultrasound, and physical measurement of parameters with the help of piezo crystals.[19] The other category includes various PCR techniques: These methods use the proliferation of the STX gene. The advantages of these methods include high sensitivity and specificity and the use of a small amount of samples for identification. However, it takes a long time to process and identify samples. They require a specialized thermocycler and specialized personnel.[20-22] Another method is the ELISA method, which is based on the binding of antibodies to the target antigen. It is a method for accurate qualitative and quantitative identification of targets from a combination of materials, but it takes a long time to identify a target.[17] The microarray technique is the next method of detection, which allows the simultaneous identification of a large number of pathogens in foods, with a simple reaction. The basic idea is that many complementary probes are joined in a matrix shape on a solid surface; each of these sites contains several copies of specific probes. The matrix is hybridized with the

DNA isolated from the sample of interest, producing a characteristic fluorescence. However, this regular microarray method needs expensive equipment, both for exploring that matrix and for compiling the generated data.[23]

Conclusion

The tracking of antigen using an immunogold labeling-based biosensor was considered as a method with high specificity, precision, speed, and could be a handy tool for the knowledge of toxic clinical strains of Shiga-like toxin-producing *E. coli* (STEC) to prevent and disease release. Accordingly, produced immunoassay-based LSPR biosensors for detection of STEC is a cost-effective plan to replace the culture methods, current methods of conventional PCR, and ELISA in isolating these bacteria from clinical specimens.

Authors' Contributions

Author contributions are similar for all of them.

Conflict of Interest Disclosures

The authors declare that they have no conflicts of interest.

Acknowledgment

The authors would like to thank the research council of Malek Ashtar Universities of Technology (MUT) for the financial support of this investigation.

References

1. Beutin L, Steinrück H, Krause G, Steege K, Haby S, Hultsch G, et al. Comparative evaluation of the Ridascreen® Verotoxin enzyme immunoassay for detection of Shiga-toxin producing strains of *Escherichia coli* (STEC) from food and other sources. J Appl Microbiol. 2007;102(3):630-9. doi:10.1111/j.1365-2672.2006.03139.x
2. Turutoglu H, Ozturk D, Guler L, Pehlivanoglu F. Presence and characteristics of sorbitol-negative *Escherichia coli* O157 in healthy sheep faeces. Vet Med. 2007;52(7):301.
3. Kargar M, Aein V, Doosti A, Gholami M, Homayoon M. Molecular Identification and Antibiotic Resistance of Shigatoxigenic *Escherichia Coli* Strains in Children of the Age of Under 5-Years with Diarrhea in Yasuj, Iran. J Isfahan Med Schl. 2014;32(273):67-78.
4. Radke SM, Alocilja EC. A high density microelectrode array biosensor for detection of *E. coli* O157: H7. Biosens Bioelectron. 2005;20(8):1662-7. doi:10.1016/j.bios.2004.07.021
5. Fratamico PM, DebRoy C. Detection of *Escherichia coli* O157: H7 in food using real-time multiplex PCR assays targeting the stx_1, stx_2, wzy_{O157}, and the $fliC_{h7}$ or eae genes. Food Anal Methods. 2010;3:330-7. doi:10.1007/s12161-010-9140-x
6. Karmali MA. Prospects for preventing serious systemic toxemic complications of Shiga toxin–producing *Escherichia coli* infections using Shiga toxin receptor analogues. J Infect Dis. 2004;189(3):355-9. doi:10.1086/381130
7. Brooks GF, Carroll KC, Butel JS, Morse SA. Jawetz, Melnick, & Adelberg's medical microbiology. McGraw-Hill Medical. Sultan Qaboos Univ Med J. 2007;7(3):273-5.
8. Smith WE, Kane AV, Campbell ST, Acheson DW, Cochran BH, Thorpe CM. Shiga toxin 1 triggers a ribotoxic stress response leading to p38 and JNK activation and induction of apoptosis in intestinal epithelial cells. Infect Immun. 2003;71(3):1497-504. doi:10.1128/iai.71.3.1497-1504.2003
9. Zeinoddini M, Azizi A, Bayat S, Tavasoli Z. Localized surface plasmon resonance (LSPR) detection of diphtheria toxoid using gold nanoparticle-monoclonal antibody conjugates. Plasmonics. 2018;13:583-90. doi:10.1007/s11468-017-0548-7
10. Faridfar G, Zeinoddini M, Akbarzedehkolahi S, Faridfar S, Nemati AS. Immunodiagnostic of *Vibrio cholerae* O1 using localized surface plasmon resonance (LSPR) biosensor. Int Microbiol. 2021;24:115-22. doi:10.1007/s10123-020-00148-8
11. Faridfar G, Zeinoddini M, Faridfar S, Saeedinia AR. LSPR-based Colorimetric Biosensor Design for Effective Immunodetection of *Vibrio Cholerae* O1. Biomacromolecular J. 2021;7(1):25-34.
12. Green RJ, Frazier RA, Shakesheff KM, Davies MC, Roberts CJ, Tendler SJ. Surface plasmon resonance analysis of dynamic biological interactions with biomaterials. Biomaterials. 2000;21(18):1823-35. doi:10.1016/S0142-9612(00)00077-6
13. Reisner DE. Bionanotechnology II: global prospects. CRC Press, 2018.
14. Dong J, Carpinone PL, Pyrgiotakis G, Demokritou P, Moudgil BM. Synthesis of precision gold nanoparticles using Turkevich method. KONA Powder Part J. 2020;37:224-32. doi:10.14356/kona.2020011
15. Yaghubi F, Zeinoddini M, Saeedinia AR, Azizi A, Samimi Nemati A. Design of localized surface plasmon resonance (LSPR) biosensor for immunodiagnostic of *E. coli* O157: H7 using gold nanoparticles conjugated to the chicken antibody. Plasmonics. 2020;15:1481-7. doi:10.1007/s11468-020-01162-2
16. Haes AJ, Hall WP, Chang L, Klein WL, Van Duyne RP. A localized surface plasmon resonance biosensor: First steps toward an assay for Alzheimer's disease. Nano lett. 2004;4(6):1029-34. doi:10.1021/nl049670j
17. Bai S, Zhao J, Zhang Y, Huang W, Xu S, Chen H, et al. Rapid and reliable detection of 11 food-borne pathogens using thin-film biosensor chips. Appl Microbiol Biotechnol. 2010;86:983-90. doi:10.1007/s00253-009-2417-6
18. van Hattum H, van der Zwaluw K, Visser GM, van Putten J, Ruijtenbeek R, Pieters RJ. Functional assay for shiga-like toxin via detection by antibody capture and multivalent galabiose binding. Bioorg Med Chem Lett. 2012;22(24):7448-50. doi:10.1016/j.bmcl.2012.10.053
19. Ivnitski D, Abdel-Hamid I, Atanasov P, Wilkins E. Biosensors for detection of pathogenic bacteria. Biosens Bioelectron. 1999;14(7):599-624. doi:10.1016/S0956-5663(99)00039-1
20. Gannon VP, King RK, Kim JY, Thomas EJ. Rapid and sensitive method for detection of Shiga-like toxin-producing *Escherichia coli* in ground beef using the polymerase chain reaction. Appl Environ Microbiol. 1992;58(12):3809-15. doi:10.1128/aem.58.12.3809-3815.1992
21. Fagan PK, Hornitzky MA, Bettelheim KA, Djordjevic SP. Detection of Shiga-like toxin (*stx1* and *stx2*), intimin (*eaeA*), and enterohemorrhagic *Escherichia coli* (EHEC) hemolysin (EHEC *hlyA*) genes in animal feces by multiplex PCR. Appl Environ Microbiol. 1999;65(2):868-72. doi:10.1128/AEM.65.2.868-872.1999

22. Subramanian S, Aschenbach KH, Evangelista JP, Najjar MB, Song W, Gomez RD. Rapid, sensitive and label-free detection of Shiga-toxin producing *Escherichia coli* O157 using carbon nanotube biosensors. Biosens Bioelectron. 2012;32(1):69-75. doi:10.1016/j.bios.2011.11.040
23. Jin HY, Tao KH, Li YX, Li FQ, Li SQ. Microarray analysis of Escherichia coli O157: H7. World J Gastroenterol. 2005;11(37):5811-5. doi:10.3748/wjg.v11.i37.5811